

Localization in Wideband SIMO Channels using Pulse Shape

Rajeev Gangula*, Omid Esrafilian†, David Gesbert† and Tommaso Melodia*

*Institute for the Wireless Internet of Things, Northeastern University, Boston, USA

†Communication Systems Department, EURECOM, Biot, France

Abstract—This work considers the problem of localization through joint angle and delay estimation in a wideband single-input multiple-output (SIMO) channel. We assume that a band-limited pulse shaping filter is used at the transmitter to convert the discrete samples into analog waveform. Majority of the prior works in localization either assume a narrowband scenario where the signal propagation delay across the receive antenna array modeled as a phase shift or neglect the pulse shaping while utilizing wideband channel models. We show that in scenarios with large bandwidth and number of antennas, changes in the amplitude of the pulse shaping waveform across the antenna array can be utilized in improving the time-of-arrival (ToA) estimation accuracy. Numerical results demonstrate that sub-meter location accuracy can be achieved at moderate bandwidths in line-of-sight (LoS) scenarios.

I. INTRODUCTION

Localizing users in a wireless network has found many applications in location-aware communication [1], navigation and autonomous vehicles [2], [3], Internet of Things (IoT), etc. Highly accurate localization is possible in 5G and beyond systems thanks to the use of massive antenna arrays and large operating bandwidths at millimeter wave and terahertz frequencies [4], [5].

In a wireless communication system with specular geometric multipath channel (MPC), the signal emitted by the transmitter (TX) arrives at the receiver (RX) via various paths. Using the pilots sent by the TX, a multi-antenna RX can estimate the distinct direction-of-arrival (DoA) and propagation delay or time-of-arrival (ToA) of each path. In this sense, channel estimation and localization are intertwined in multi-antenna wireless channels having specular multipath. While the angular resolution increases with the number of antennas, the delay resolution increases with the operating bandwidth of the system.

The channel estimation and/or localization by evaluating the MPC parameters in multi-antenna scenarios is studied in [6]–[16]. While the works in [6]–[10] estimate the angles and delays using compressive sensing and dictionary based strategies, the works in [11]–[16] are non-dictionary based and provide direct solutions based on the problem structure. In the former class of methods, joint angle and delay estimation (JADE) problem can be formulated to find the DoA and ToA in MPC. To solve the JADE problem, maximum likelihood based (ML) estimators are derived in [11], 2D-subspace methods are proposed in [12], [13], and 2D-Matrix pencil algorithms using a single snapshot can be found in [17].

The existing works in localization or JADE have two common assumptions.

- The transmitted signal is of narrowband and the RX is equipped with a phased antenna array spaced at half wavelength or closer. When the number of antennas are small, this scenario entails that the delay across the antenna array can be modeled as a phase shift. We term this as narrowband assumption in this paper.
- Non band-limited channel model is used where the multipaths are represented by Dirac delta function while ignoring the baseband pulse-shaping effects. Typically raised-cosine filters are used for pulse-shaping in digital modulation at the TX.

In the regime of large system bandwidth and the number of antennas at the RX, as pointed out in [18], [19], the narrowband assumption is not valid as the path delay varies considerably across the antenna array. This phenomena is termed as spatial wideband effect. The works [18]–[20] in explore the optimization methods to find the angle and delay of the multipath components while utilizing the spatial wideband channel model. However, all these works ignore the baseband pulse-shaping filtering effects at the TX. The authors in [6] consider the band-limited channel model where the effects of pulse-shaping is included, however, ignores the spatial wideband effects.

In this work, we consider the localization through JADE in a SIMO system where both the spatial wideband and band-limited conditions are captured in the channel model. We show that ToA and DoA estimation accuracy can be considerably improved by exploiting the changes in amplitude of the received baseband pulse-shaping waveform across the RX antenna array.

II. SYSTEM MODEL

We consider a L tap wideband single-input multiple-output (SIMO) channel. The receiver (RX) is equipped with N antenna uniform linear array (ULA) while the transmitter (TX) has a single antenna. Assuming a specular multipath scenario, a geometric channel model consisting of P paths is considered. The channel coefficient of the l -th tap at the i -th $i \in [1, N]$ RX antenna is given by

$$h_{i,l} = \sum_{p=1}^P g_p s[lT_s - \tau_{i,p}], l \in [1, L], \quad (1)$$

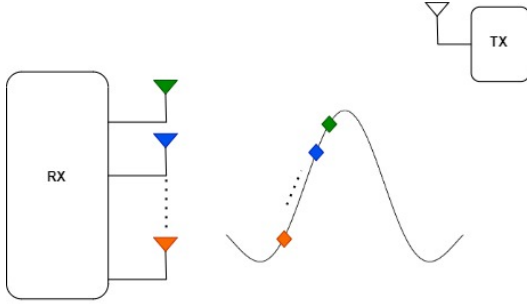


Figure 1: Rx waveform and sampled values in noiseless scenario.

where $g_p \in \mathbb{C}$ is the path gain, $\tau_{i,p}$ is the path delay, sampling interval $T_s = 1/W$, W is the system bandwidth and $s[\cdot]$ is the baseband pulse shaping function. Typically raised-cosine functions are used to represent $s[\cdot]$.

We assume that the RX has access to noisy channel estimate

$$\mathbf{y}_l = \mathbf{h}_l + \mathbf{w}_l, \quad (2)$$

$$\mathbf{h}_l = [h_{1,l}, h_{2,l}, \dots, h_{N,l}]^T \in \mathbb{C}^{N \times 1}, l \in [1, L],$$

and $\mathbf{w}_l \in \mathbb{C}^{N \times 1}$ is the i.i.d. complex circular symmetric additive Gaussian noise. The channel estimation is usually accomplished sending pilot or training symbols.

The TX and RX lie on a 2-D plane, and let θ_p , $p \in [1, P]$ denote the direction-of-arrival (DoA) of the p -th path. When the antenna element spacing d is much smaller than the distance travelled by the path, under the plane wave propagation assumption, the propagation delay across antenna elements can be approximated as

$$\tau_{i,p} \approx \tau_{1,p} + (i-1)(d/c) \sin(\theta_p), \quad i \in [2, N],$$

where $\tau_{1,p}$ denotes propagation delay at the first antenna element and c is the speed of light. The l -th tap antenna response can then be written as

$$\mathbf{h}_l = \sum_{p=1}^P g_p \mathbf{a}_l(\theta_p, \tau_{1,p}), \quad (3)$$

where the space-time steering vector $\mathbf{a}_l(\theta_p, \tau_{1,p})$ is given by

$$\mathbf{a}(\theta_p) \text{diag} \begin{bmatrix} s(lT_s - \tau_{1,p}) \\ s(lT_s - \tau_{1,p} - d \sin(\theta_p)/c) \\ \vdots \\ s(lT_s - \tau_{1,p} - (N-1)d \sin(\theta_p)/c) \end{bmatrix}, \quad (4)$$

and $\mathbf{a}(\theta_p) = [1 e^{-j2\pi d \sin(\theta_p)/\lambda} \dots e^{-j2\pi(N-1)d \sin(\theta_p)/\lambda}]^T$.

A. Wideband Vs Narrowband

Majority of previous works in channel estimation or joint angle and delay estimation (JADE) utilize a narrowband channel model. They assume that the RX waveform doesn't change significantly across the antenna array. This results in the approximation $s(t - \tau_{i,p}) \approx s(t - \tau_{1,p})$, $\forall i$. In this scenario, the second term in the space-time steering vector in (4) becomes a scalar. The differential delay across the antennas results in

only phase difference and the effect is captured in the steering vector $\mathbf{a}(\theta_p)$. The $\text{diag}(\cdot)$. The narrowband assumption is valid when a) $s(\cdot)$ is narrowband i.e., $\tau_{i,p} \ll 1/W, \forall i, \forall p$, and b) the time taken by the signal to propagate over the entire antenna array satisfies $\tau_{i,p} < D\lambda/c, \forall i, \forall p$ where D denotes the aperture of the antenna array in wavelengths λ . Based on the above conditions, the narrowband assumption is justified when

$$W \ll c/\lambda D.$$

Consider a typical 5G system operating at 2 GHz carrier over a bandwidth of 80 MHz, and RX is equipped with a 32 element ULA with half-wavelength spacing. In this scenario we can clearly see that the assumption $W(80) \ll c/\lambda D(125)$ doesn't hold. Therefore, in this paper, we consider the wideband channel model.

B. Data model

To perform JADE, various observations of the noisy channel estimates are collected. By stacking the columns of the measurements in (2), we have

$$\mathbf{y} = \begin{bmatrix} \mathbf{h}_1 \\ \mathbf{h}_2 \\ \vdots \\ \mathbf{h}_L \end{bmatrix} + \begin{bmatrix} \mathbf{w}_1 \\ \mathbf{w}_2 \\ \vdots \\ \mathbf{w}_L \end{bmatrix}. \quad (5)$$

From (3) and (5), we have $\mathbf{y} \in \mathbb{C}^{NL \times 1}$

$$\mathbf{y} = \mathbf{A}(\boldsymbol{\theta}, \boldsymbol{\tau})\mathbf{g} + \mathbf{w}, \quad (6)$$

with $\mathbf{A}(\boldsymbol{\theta}, \boldsymbol{\tau}) = [\tilde{\mathbf{a}}(\theta_1, \tau_{1,1}), \tilde{\mathbf{a}}(\theta_2, \tau_{1,2}), \dots, \tilde{\mathbf{a}}(\theta_P, \tau_{1,P})]$,

$$\tilde{\mathbf{a}}(\theta_p, \tau_{1,p}) = \begin{bmatrix} \mathbf{a}_0(\theta_p, \tau_{1,p}) \\ \mathbf{a}_1(\theta_p, \tau_{1,p}) \\ \vdots \\ \mathbf{a}_{L-1}(\theta_p, \tau_{1,p}) \end{bmatrix},$$

$\mathbf{w} = [\mathbf{w}_1, \mathbf{w}_2, \dots, \mathbf{w}_L]^T$, and $\mathbf{g} = [g_1, g_2, \dots, g_P]^T$.

We assume that M such independent channel estimate measurements are available, given by

$$\mathbf{Y} = [\mathbf{y}^{(1)}, \mathbf{y}^{(2)}, \dots, \mathbf{y}^{(M)}],$$

where the m -th observation

$$\mathbf{y}^{(m)} = \mathbf{A}(\boldsymbol{\theta}, \boldsymbol{\tau})\mathbf{g}^{(m)} + \mathbf{w}^{(m)}, \quad m \in [1, M],$$

$\mathbf{g}^{(m)}$ is the channel gain and $\mathbf{w}^{(m)}$ is the noise of the m -th observation.

For localization purposes we seek to jointly estimate the parameters $(\theta_p, \tau_{1,p}) \forall p \in [1, P]$. This can be achieved by using the observations in \mathbf{Y} and the known structure of the space-time matrix $\mathbf{A}(\boldsymbol{\theta}, \boldsymbol{\tau})$. Some assumptions regarding the space-time matrix are stated below.

- A path having a unique pair of $(\theta_p, \tau_{1,p})$ results in unique space-time vector $\tilde{\mathbf{a}}(\theta_p, \tau_{1,p})$. This leads to a space-time manifold having no ambiguities.

- The space-time matrix $\mathbf{A}(\boldsymbol{\theta}, \boldsymbol{\tau})$ is tall with $NL > P$. In case of all distinct paths, $\mathbf{A}(\boldsymbol{\theta}, \boldsymbol{\tau})$ has a full column rank.
- The number of paths P is known.
- The pulse-shaping waveform $s(\cdot)$ is known to the RX.

III. PROBLEM FORMULATION

If the path gains are treated as unknown deterministic parameters, and the noise being white Gaussian, the maximum likelihood approach results in the following optimization problem:

$$\begin{aligned} \min_{\boldsymbol{\tau}, \boldsymbol{\theta}, \mathbf{G}} \quad & \|\mathbf{Y} - \mathbf{A}(\boldsymbol{\theta}, \boldsymbol{\tau})\mathbf{G}\|^2 \\ \text{subject to} \quad & -\pi/2 \leq \theta_p \leq \pi/2, \quad p \in [1, P], \\ & 0 \leq \tau_{1,p} \leq LT_s, \quad p \in [1, P], \end{aligned}$$

where $\mathbf{G} = [\mathbf{g}^{(1)}, \mathbf{g}^{(2)}, \dots, \mathbf{g}^{(M)}]$.

It is well known that this optimization problem is separable and reducible to optimization parameters of interest, angles and delays.

$$(\boldsymbol{\theta}^*, \boldsymbol{\tau}^*) = \arg \max_{\boldsymbol{\theta}, \boldsymbol{\tau}} \text{tr} \mathbf{P}_A \mathbf{R}_y \quad (7)$$

where $\mathbf{P}_A = \mathbf{A}(\mathbf{A}^* \mathbf{A})^{-1} \mathbf{A}^*$ and $\mathbf{R}_y = \mathbf{Y}\mathbf{Y}^*/M$, and $(\cdot)^*$ denotes the complex-conjugate transpose. This is a non-convex problem and solving this still requires a search over $2P$ dimensional space which becomes prohibitively complex even for small values of P . We now present a suboptimal approach based on 2D-MUSIC algorithm which requires only a two-dimensional search.

A. 2D-MUSIC

MUSIC algorithm relies on the fact that the space-time steering vector $\tilde{\mathbf{a}}(\theta_p, \tau_{1,p})$ is orthogonal to the noise subspace \mathbf{Q} . The noise subspace matrix \mathbf{Q} is formed by the eigenvectors of \mathbf{R}_y corresponding to the $NL - P$ smallest eigenvalues. The peaks in the 2D MUSIC spectrum

$$P_{\text{music}}(\theta_p, \tau_{1,p}) = \frac{\|\tilde{\mathbf{a}}(\theta_p, \tau_{1,p})\|^2}{\|\mathbf{Q}\tilde{\mathbf{a}}(\theta_p, \tau_{1,p})\|^2}, \quad (8)$$

corresponds to the multipath delays and angles $(\theta_p, \tau_{1,p})$.

IV. LOS SCENARIO

In this section we consider a scenario where there is only a line-of-sight (LoS) path. We also assume that RX has access to only one observation of the noisy channel estimate unlike in the previous section. Subspace methods like 2D MUSIC hence can't be applied in this scenario. Generally ToA is estimated using peak detection methods, where the first detected peak with sufficient energy in the channel impulse response corresponds to the LoS path. The aim of this work is to showcase the improvement in ToA resulting from the pulse-shape information rather than revisit the existing ToA estimation methods. Therefore, we assume that there is a ToA estimation block (using existing methods) that can perfectly predict the indices of taps that carry significant energy from

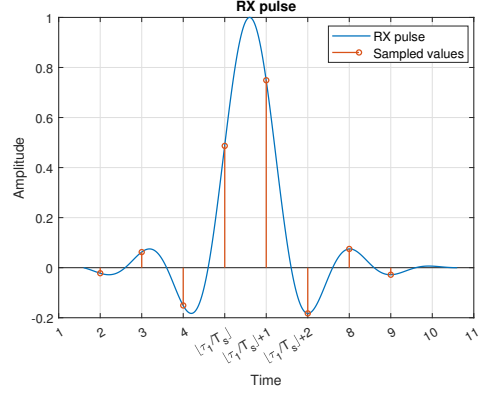


Figure 2: Rx waveform and sampled values in noiseless scenario.

the LoS path. This block outputs the tap indices $\{l_1, l_2\}$, where $l_1 = \lfloor \tau_{1,1}/T_s \rfloor$ and $l_2 = \lfloor \tau_{1,1}/T_s \rfloor + 1$. An illustration of this for a noiseless scenario is shown in Figure 2. With perfect peak detection we are able to estimate the delay from the TX to the first antenna of the RX, $\tau_{1,1}$ with an error up to $T_s/2$. Now we focus on improving this baseline performance by using the pulse-shape information.

The stacked channel estimate response vector of the l_1 and l_2 -th tap can be written as

$$\begin{bmatrix} \mathbf{y}_{l_1} \\ \mathbf{y}_{l_2} \end{bmatrix} = g_1 \begin{bmatrix} \mathbf{a}_{l_1}(\theta_1, \tau_{1,1}) \\ \mathbf{a}_{l_2}(\theta_1, \tau_{1,1}) \end{bmatrix} + \begin{bmatrix} \mathbf{w}_{l_1} \\ \mathbf{w}_{l_2} \end{bmatrix}, \quad (9)$$

where $\mathbf{a}_{l_1}(\theta_1, \tau_{1,1})$ and $\mathbf{a}_{l_2}(\theta_1, \tau_{1,1})$ are the space-time steering vectors for taps l_1 and l_2 , respectively. Using (9), the maximum likelihood estimation of ToA and DoA can then be obtained by solving

$$\min_{\tau_{1,1}, \theta_1, g_1} \left\| \begin{bmatrix} \mathbf{y}_{l_1} \\ \mathbf{y}_{l_2} \end{bmatrix} - g_1 \begin{bmatrix} \mathbf{a}_{l_1}(\theta_1, \tau_{1,1}) \\ \mathbf{a}_{l_2}(\theta_1, \tau_{1,1}) \end{bmatrix} \right\|^2 \quad (10a)$$

$$\text{subject to} \quad -\pi/2 \leq \theta \leq \pi/2, \quad (10b)$$

$$(l_1 - 1)T_s \leq \tau_1 \leq (l_2 + 1)T_s, \quad (10c)$$

where the constraint in (10b) covers the range of DoAs. Since we do not know the DoA in advance, the sign of the differential delay $d \sin(\theta)/c$ is unknown. Hence, we need to search across both sides of the taps l_1 and l_2 . As the pulse $s(\cdot)$ typically has most of its energy concentrated in neighbourhood taps we restrict the search from $l_1 - 1$ to $l_2 + 1$. This is reflected in the constraint (10c).

The solution to (10) is a well known matched filter [21]. Optimal values of $\tau_{1,1}$ and θ_1 are obtained by solving

$$(\tau_{1,1}^*, \theta_1^*) = \max_{\tau_{1,1}, \theta_1} \frac{\left| \begin{bmatrix} \mathbf{a}_{l_1}(\theta_1, \tau_{1,1})^H & \mathbf{a}_{l_2}(\theta_1, \tau_{1,1})^H \end{bmatrix} \begin{bmatrix} \mathbf{y}_{l_1} \\ \mathbf{y}_{l_2} \end{bmatrix} \right|^2}{\left\| \begin{bmatrix} \mathbf{a}_{l_1}(\theta_1, \tau_{1,1}) \\ \mathbf{a}_{l_2}(\theta_1, \tau_{1,1}) \end{bmatrix} \right\|^2}, \quad (11)$$

subject to constraints (10b) and (10c).

V. NUMERICAL RESULTS

Numerical simulations are performed to demonstrate the advantages of using wideband channel model for JADE.

We assume that the system operates over a bandwidth of $W = 80$ MHz at a carrier frequency $f_c = 3$ GHz. Both the TX and the RX are located in the x-y plane. The RX has a ULA with $N = 32$ antennas. The i -th antenna placed at the coordinate $(0, (i - 1)d\lambda/2), i \in [1, N]$.

A. Multipath Scenario

A total number of $P = 5$ paths is considered with DoA $\theta = [-60^\circ - 59^\circ - 61^\circ 60^\circ 30^\circ]$ and delays $\tau = [1.35 1.1 1.2 2.8 2.5] * T_s$. Raised cosine pulse is used for pulse-shaping. The path gains $g_p \sim \mathcal{CN}(0, 1/P), \forall p$. Figures 3 and 4 illustrate the 2D-MUSIC spectrum for narrowband and wideband system model, respectively. To construct the subspace matrix 100 observations are used. The SNR is 15 dB. It can be clearly seen that the wideband model is able to resolve the closely spaced multipath components while the narrowband model fails.

B. LoS Scenario

In this scenario we assume that there exist only LoS path. The RX is located origin with the i -th antenna coordinate being $(0, (i - 1)d\lambda/2), i \in [1, N]$. The TX is located at a distance of r meters and at an angle θ from the origin. The channel gain $g \in \mathbb{C}$ follows normal distribution. The range error derived from TOA estimation is show in Figure 5 while that of DoA is shown in 6. It can be seen that range error drastically reduces when we apply the wideband model. The range error reduction stems from the fact that the wideband model exploits the pulse shape information. In the simulation, we assume that the peak detector is perfect and always able to detect the peak located at either $\lceil \tau_{1,1}/T_s \rceil$ or $\lceil \tau_{1,1}/T_s \rceil + 1$.

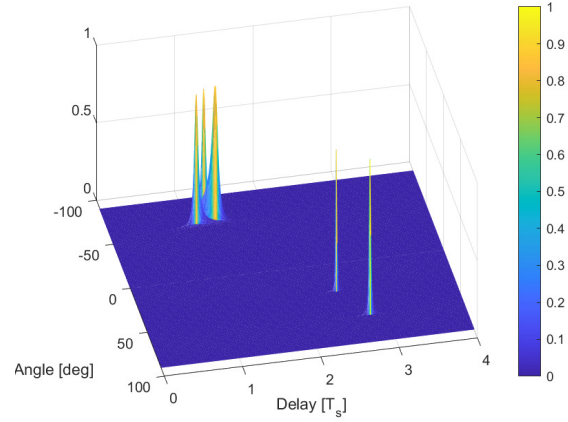


Figure 4: Range error for different SNRs.

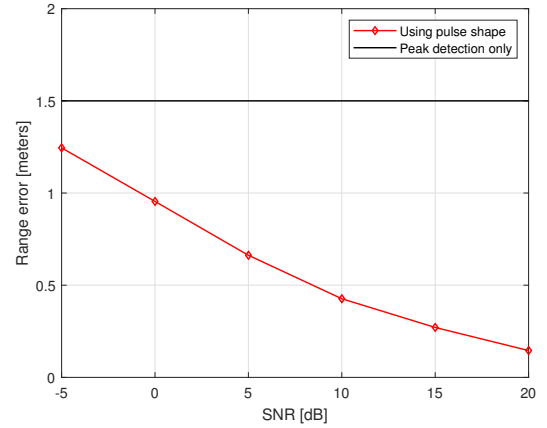


Figure 5: Range error for different SNRs.

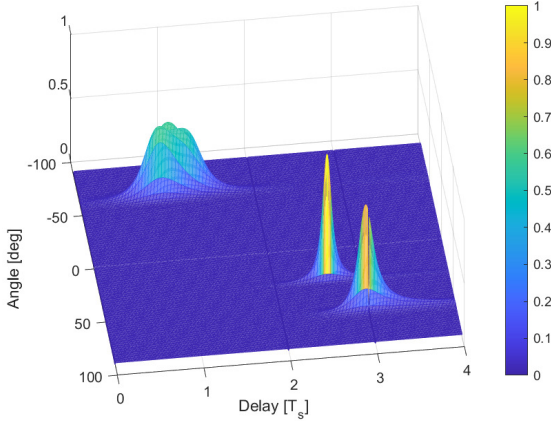


Figure 3: Range error for different SNRs.

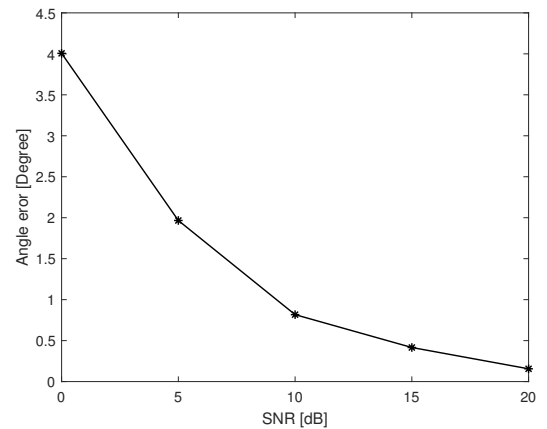


Figure 6: Angle error for different SNRs.

For peak detection only scheme, error is calculated as $\min\{\tau_{1,1} - \lceil \tau_{1,1}/T_s \rceil, \tau_{1,1} - \lceil \tau_{1,1}/T_s \rceil - 1\}$.

REFERENCES

- [1] A. Conti, F. Morselli, Z. Liu, S. Bartoletti, S. Mazuelas, W. C. Lindsey, and M. Z. Win, "Location awareness in beyond 5G networks," *IEEE Communications Magazine*, vol. 59, no. 11, pp. 22–27, 2021.
- [2] A. Abdallah, J. Khalife, and Z. M. Kassas, "Exploiting on-demand 5G downlink signals for opportunistic navigation," *IEEE Signal Processing Letters*, vol. 30, pp. 389–393, 2023.
- [3] R. Karlsson and F. Gustafsson, "The future of automotive localization algorithms: Available, reliable, and scalable localization: Anywhere and anytime," *IEEE Signal Processing Magazine*, vol. 34, no. 2, pp. 60–69, 2017.
- [4] H. Chen, H. Srieddeen, T. Ballal, H. Wymeersch, M.-S. Alouini, and T. Y. Al-Naffouri, "A tutorial on terahertz-band localization for 6g communication systems," *IEEE Communications Surveys Tutorials*, vol. 24, no. 3, pp. 1780–1815, 2022.

- [5] F. Wen, H. Wymeersch, B. Peng, W. P. Tay, H. C. So, and D. Yang, "A survey on 5g massive mimo localization," *Digital Signal Processing*, vol. 94, pp. 21–28, 2019.
- [6] W. Zheng and N. González-Prelcic, "Joint position, orientation and channel estimation in hybrid mmwave mimo systems," in *2019 53rd Asilomar Conference on Signals, Systems, and Computers*, 2019.
- [7] A. Shahmansoori, G. E. Garcia, G. Destino, G. Seco-Granados, and H. Wymeersch, "Position and orientation estimation through millimeter-wave mimo in 5g systems," vol. 17, no. 3, 2018, pp. 1822–1835.
- [8] J. Talvitie, M. Koivisto, T. Levanen, M. Valkama, G. Destino, and H. Wymeersch, "High-accuracy joint position and orientation estimation in sparse 5g mmwave channel," in *ICC 2019 - 2019 IEEE International Conference on Communications (ICC)*, 2019.
- [9] K. Venugopal, A. Alkhateeb, N. González Prelcic, and R. W. Heath, "Channel estimation for hybrid architecture-based wideband millimeter wave systems," *IEEE Journal on Selected Areas in Communications*, vol. 35, no. 9, pp. 1996–2009, 2017.
- [10] X. Wu, G. Yang, F. Hou, and S. Ma, "Low-complexity downlink channel estimation for millimeter-wave fdd massive mimo systems," *IEEE Wireless Communications Letters*, vol. 8, no. 4, pp. 1103–1107, 2019.
- [11] M. Wax and A. Leshem, "Joint estimation of time delays and directions of arrival of multiple reflections of a known signal," *IEEE Transactions on Signal Processing*, vol. 45, no. 10, pp. 2477–2484, 1997.
- [12] M. Vanderveen, C. Papadias, and A. Paulraj, "Joint angle and delay estimation (JADE) for multipath signals arriving at an antenna array," *IEEE Communications Letters*, vol. 1, no. 1, pp. 12–14, 1997.
- [13] A.-J. van der Veen, M. Vanderveen, and A. Paulraj, "Joint angle and delay estimation using shift-invariance techniques," *IEEE Transactions on Signal Processing*, vol. 46, no. 2, pp. 405–418, 1998.
- [14] J. Zhang and M. Haardt, "Channel estimation and training design for hybrid multi-carrier mmwave massive MIMO systems: The beamspace ESPRIT approach," in *2017 25th European Signal Processing Conference (EUSIPCO)*, 2017, pp. 385–389.
- [15] A. Liao, Z. Gao, H. Wang, S. Chen, M.-S. Alouini, and H. Yin, "Closed-loop sparse channel estimation for wideband millimeter-wave full-dimensional MIMO systems," *IEEE Transactions on Communications*, vol. 67, no. 12, pp. 8329–8345, 2019.
- [16] F. Wen, J. Kulmer, K. Witrissal, and H. Wymeersch, "5g positioning and mapping with diffuse multipath," *IEEE Transactions on Wireless Communications*, vol. 20, no. 2, pp. 1164–1174, 2021.
- [17] A. Bazzi, D. T. M. Slock, and L. Meilhac, "Single snapshot joint estimation of angles and times of arrival: A 2d matrix pencil approach," in *2016 IEEE International Conference on Communications (ICC)*, 2016, pp. 1–6.
- [18] B. Wang, M. Jian, F. Gao, G. Y. Li, and H. Lin, "Beam squint and channel estimation for wideband mmwave massive mimo-ofdm systems," *IEEE Transactions on Signal Processing*, vol. 67, no. 23, pp. 5893–5908, 2019.
- [19] B. Wang, F. Gao, S. Jin, H. Lin, and G. Y. Li, "Spatial- and frequency-wideband effects in millimeter-wave massive mimo systems," *IEEE Transactions on Signal Processing*, vol. 66, no. 13, pp. 3393–3406, 2018.
- [20] S. Weng, F. Jiang, and H. Wymeersch, "Wideband mmwave massive mimo channel estimation and localization," *IEEE Wireless Communications Letters*, vol. 12, no. 8, pp. 1314–1318, 2023.
- [21] E. Tuncer and B. Friedlander, *Classical and modern direction-of-arrival estimation*. Academic Press, 2009.